ELSEVIER

Polymer 41 (2000) 1087–1098

polymer

Characterization of low molecular weight poly(β-hydroxybutyrate)s from alkaline and acid hydrolysis

Ga-er Yu, R.H. Marchessault*

Department of Chemistry and Pulp and Paper Research Centre, McGill University, 3420 University Street, Montreal, Quebec, Canada H3A 2A7

Received 22 January 1999; received in revised form 18 March 1999; accepted 19 March 1999

Abstract

In the present paper, low molecular weight poly(β-hydroxybutyrates) (PHBs), which were obtained by acidic and basic hydrolysis of bacterially produced PHB, were characterized by gel permeation chromotography (GPC), ^{1}H, ^{13}C and ^{31}P NMR. The assignments of the resonances of ^{13}C NMR spectra from unsaturated end and hydroxy end groups were made using heteronuclear multiple quantum coherence (HMQC) NMR technique. Unsaturation contents and number average molecular weights of the PHBs were determined mainly by ^{1}H and ^{31}P NMR. Direct measurement of the molecular weights of PHB has also been carried out by matrix assisted laser desorption ionization (MALDI). Based on the characterization of these low molecular weight PHBs, the heterogeneous hydrolysis mechanism is discussed and the scission of PHB chains is proposed to occur at the surfaces and interfaces of lamellar crystals. The unsaturated end group is formed by dehydration of the chain ends by β-elimination after ester hydrolysis, which is different from the mechanistic steps of the formation of unsaturated ends in thermal decomposition of PHB. The correlation of thickness of crystal lamellae and the melting points has also been discussed. The plot of the melting point against reciprocal lamellar thickness for low molecular weight PHB indicates the pronounced effect of the surface energy of these crystals, which is caused by the large proportion of end groups. © 1999 Elsevier Science Ltd. All rights reserved.

Keywords: Low molecular weight poly(β-hydroxybutyrate); Heterogeneous hydrolysis mechanism; Lamellar thickness

1. Introduction

Progress in understanding the structure–property relation of bacterially produced poly(3-hydroxybutyrate), PHB, and its copolymers, e.g. poly(3-hydroxybutyrate/valerate), PHB/V, is summarized in recent reviews [1–10] and conference proceedings [11,12]. Bacterial PHBs can have molecular weights ranging from 10^6–10^7 and are optically active, aliphatic polyesters. PHB is a highly crystalline material with melting point around 180°C. The basic structure of PHB is shown in Scheme 1.

PHB is well known as a biodegradable and biocompatible polymer, see Ref. [9]. PHB and its copolymers are degraded by purified bacterial enzymes [13–17]. The mechanism of this heterogeneous enzymatic degradation of PHB and its copolymers has been developed by using folded chain single crystals as model substrates [17–23]. The observed splintering of the single crystals is in keeping with a mechanism [22] where enzymes 'shave off' the molecular chains parallel to the chain folding plane at the edge of a lath-shaped PHB crystal. Accordingly, the residual PHB retains the same molecular weight as before the degradation. The chain scission proceeds by both *endo* and *exo* action to solubilize the edge material and the overall effect is called "processive degradation" [22,23]. This mechanism applied to highly ordered single crystals explains the unusual splintering of the crystals into folded chain lamellae with an axial ratio of 100–200 [22].

The mechanisms of thermal degradation of PHB and its copolymers are sensitive to the investigated temperature range. At moderate temperatures, it is widely accepted that the PHB is decomposed through a random scission process involving a six-membered ring ester intermediate, or β-elimination [24–32] as illustrated in Scheme 2.

This mechanism gives almost exclusively unsaturated ends for the products. Investigation on the thermal decomposition of PHB to cyclics has also been carried out by Hoecker's group [33].

PHB can also be hydrolysed in acidic and basic conditions, as a normal ester, in the ways shown in Scheme 3 [34]. The hydrolysis by base is known as *saponification* and was first reported by Lemoigne who used the result as a proof of the chemical structure of the PHB chain [35].

* Corresponding author. Fax: +1-514-398-7249.
E-mail address: ch21@musica.mcgill.ca (R.H. Marchessault)

0032-3861/00/$ - see front matter © 1999 Elsevier Science Ltd. All rights reserved.
PII: S0032-3861(99)00230-X

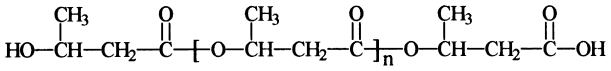

Scheme 1.

Hydrolytic degradation of PHB and its copolymers have been studied both in vivo and in vitro [36–44]. The results show that the high molecular weight PHB and PHB/V degrade relatively slowly at physiological pH values (7.0–7.4). A random scission of the polymer chains occurs first followed by weight loss of the samples caused by further decomposition [42,43]. Hydrolysis of PHB by a strong acid (3 N HCl) at 104.5°C [45] showed that the acid attacks the ester linkages of both the crystalline shell and the non-crystalline core of the PHB granules.

Recent publications from Braud et al [46,47] have focused on the analysis of the water soluble products or PHB oligomers from hydrolysis of PHB catalysed by *p*-toluene sulfonic acid at 70°C in 1,2-dichloroethane for 10 h. They used capillary zone electrophoresis (CZE), which is sensitive to ions, to separate and detect the oligomers of 2–7 units. Crotonic acid and oligomers with unsaturated ends were detected. With further aging, the aqueous solutions (phosphate buffer pH 6.8) of the oligomers at different temperature, they found that more unsaturated ends were formed via a dehydration process from the oligomers.

Hydrolysis of PHB in base conditions and precipitation fractionation of the hydrolytic products were carried out by Hauttecoeur et al. [48–53] They used NaOH to degrade PHB in CH_3OH. Fractionation was carried out using $CH_3CH_2OH/CHCl_3$ in different proportions. Low molecular weight PHB fractions with narrow melting point ranges were obtained.

Welland et al. [54] used gaseous methylamine to selectively etch the lamellar surfaces of PHB single crystals via a chain scission reaction as shown in Scheme 4. Low molecular weight products with double peaks (molecular weight related by a factor of 2) from GPC analysis were always observed, which indicated there were 'buried folds' in the single crystals of PHB, which did not respond to the chain scission reagent.

Low molecular weight PHB or PHB oligomers are useful [45] for the preparation of specialty graft and block

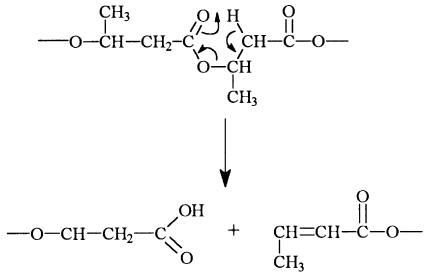

Scheme 2.

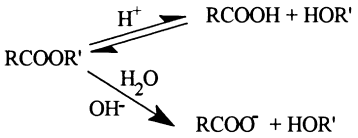

Scheme 3.

copolymers. Recently, grafting PHB onto chitosan [55] and synthesis of amphiphilic block copolymers of PHB with poly(oxyethylene) [56] have been reported based on low molecular weight PHB. Clearly, it is important to understand the structure–property relationships of low molecular weight PHB, before the properties of graft copolymers or block copolymers are explored. Melting points and the thicknesses of lamellae of some low molecular weight PHBs have been studied in our laboratory. [57] High pressure liquid chromatography [58] has successfully been used to separate and analyse oligomers of low molecular weight PHB. ^{31}P NMR [59] has also been used to determine the unsaturated contents and molecular weights for PHBs. In this paper, we will use ^{1}H, ^{13}C, ^{31}P NMR techniques to characterize the end groups and molecular weights for a few low molecular weight PHBs, which were prepared and kindly donated by Hauttecoeur [48–53]. GPC and matrix assisted laser desorption ionization (MALDI) are used to detect the molecular weights and molecular weight distributions (M_w/M_n). Based on these analyses, we will further discuss the mechanisms of hydrolysis of PHB. Some previous data [57] of melting points and lamellar thicknesses are combined in the present paper for further discussion.

2. Experimental

2.1. Materials

A few low molecular weight PHB samples used in this study were kindly donated by B. Hauttecoeur formerly of the Institut Pasteur, Paris. These low molecular weight samples of PHB were prepared by Hauttecoeur et al. using a base hydrolysis method: PHB dissolved in $CHCl_3$ was precipitated with methanol from a 4% solution and washed extensively in methanol. NaOH was added to the methanol suspension of PHB and base hydrolysis was performed at low temperatures (−18 or −24°C) for various lengths of time. The hydrolysed product was fractionated in ethanol/$CHCl_3$ [48]. High molecular weight bacterial PHB (BX G08, $M_w \sim 174\,000$) was a gift from ICI. A low molecular

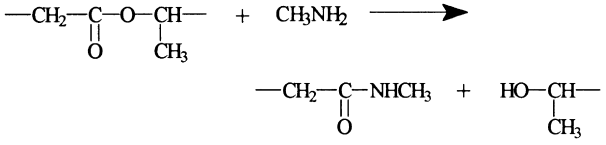

Scheme 4.

weight PHB sample was prepared by hydrolysis of a PHB sample (BX G08) at 104°C in 3 N HCl for 15 h. After the hydrolysis, the insoluble phase was filtered and washed with excess of deionized water. The product was dried under vacuum. Observation by scanning electron microscopy (SEM) of this product showed that it had the shape of spray-dried native granules of BX G08 sample, which agreed with previous studies [45].

2.2. Gel permeation chromatography

GPC experiments provided the relative molecular weights and the molecular weight distributions of the PHB samples studied presently. All the GPC experiments were performed at room temperature. Three GPC systems have been used. The first GPC system was run with dioxane as eluent at a flow rate of 1 $cm^3\,min^{-1}$. Six Waters styragel columns were used: HMW 6E, HR 5E, HR4, HR 3, HR 1 and HR 0.5. A Hewlett–Packard refractive index detector (HP 1047A RI detector) was used. The second GPC system used tetrahydrofuran (THF) as eluent at a flow rate of 0.6 $cm^3\,min^{-1}$ and a Varian RI-4 refractive index detector was employed. Two columns (styragel HR 4 and HR 1) were used. The third GPC system was run with $CHCl_3$ as eluent at a flow rate of 1 $cm^3\,min^{-1}$. Four Phenomenex columns were used: three 5 μ500A and one 5 linear. A UV detector was set to record at $\lambda = 254$ nm.

2.3. Nuclear magnetic resonance

^{1}H NMR experiments were carried out on either a Varian Unity 500 or a Varian Gemini 200 at 500 or 200 MHz, respectively. ^{13}C NMR experiments were performed on either a Varian Unity 500 or a Varian XL 300 at 125 and 75 MHz, respectively. A sample was dissolved in $CDCl_3$ with a concentration of about 0.2–2 wt%, depending on whether ^{1}H or ^{13}C NMR spectra were recorded. For 1D ^{1}H NMR spectra, relaxation delay time $d1 = 6$ s were used with a flip angle 45–75°. For 1D ^{13}C NMR spectra, relaxation delay time $d1 = 12$–14 s were used with 70–90° pulse. Correlation spectroscopy (COSY) and heteronuclear multiple quantum coherence (HMQC) 2D spectra were recorded on Unity 500. Relaxation delay time, $d1 = 4$–6 s and $d1 = 6$ s for COSY and HMQC experiments was used, respectively. Null time = 0.4 s for HMQC experiments was used because it was suitable for major resonances.

^{31}P NMR experiments were carried out with a Varian XL 300 at 121 MHz. The parameters used were similar to those in a previous paper [59], a 30-s delay time was used and 32–128 scans were performed for each solution. The concentrations of all the solutions for ^{31}P NMR experiments were accurately determined by weight. A sample was dissolved in $CDCl_3$ with concentration about 2 wt%, then the internal standard solution of bisphenol A (BPA) in pyridine (4.8 wt%) with a relaxation agent $Cr(acac)_3$ (0.2 wt%) was added. Excess amount of phosphorous agent 2-chloro-4,4,5,5-tetramethyldiozaphospholane was added to the mixture, using a calibrated syringe, to react with –OH and –COOH functional groups.

2.4. Differential scanning calorimetry

Differential scanning calorimetry (DSC) experiments were performed on a Perkin–Elmer DSC-7 for measurement of melting points and heat of fusion for a few PHB samples. Melting point and the heat of fusion from Indium were used for the calibration. The heating rate was 10° min^{-1}.

2.5. Matrix assisted laser desorption ionization time-of-flight

MALDI-TOF mass spectra were recorded on a Kratos Kompact MALDI-III TOF mass spectrometer with the instrument set in the positive reflection mode. 1,8,9-anthracenetriol (dithranol) was used as the matrix. The matrix solution was prepared by dissolving dithranol in $CHCl_3$ (10 mg ml^{-1}). The ionizing agent LiBr was dissolved in THF (10 mg ml^{-1}). A PHB sample was dissolved in $CHCl_3$ (5 mg ml^{-1}). The solution for the analysis was prepared from mixing one portion of the sample solution with two portions of the matrix solution and one portion of the LiBr solution. One drop of the mixed solution was applied to a stainless sample slide and air dried. More detailed procedure on the instrument set-up and the experimental conditions can be found in Ref. [60].

3. Results and discussion

3.1. Solubility of the samples

Solubility of the bacterial PHB is poor in many common organic solvents, due to its high molecular weight and high crystallinity. Recently, 3D solubility parameters have been calculated based on Hansen's method to classify solvents for PHB [61]. In the present study, it is found experimentally that low molecular weight PHB could be dissolved in dioxane and THF, so that the low molecular weight PHB could be analysed in dioxane and THF by GPC. Dioxane is a partial solvent for PHB from the calculations [61].

3.2. NMR analysis

^{1}H and ^{13}C NMR spectra of high molecular weight PHB have been studied by several groups, for example, see Refs [62–68]. In this paper, we are mainly concerned with the end groups of PHB. ^{1}H NMR spectra for low molecular weight PHB samples have been assigned using synthesized model compounds [68] and from pyrolysis products [29,30]. In the present study, we have used the COSY technique to confirm the ^{1}H NMR assignments for PHB end groups. Further, we have used the HMQC technique to assign the end groups from PHB in ^{13}C NMR spectra. For clarity, the spectra from HMQC experiments are plotted in three spectra

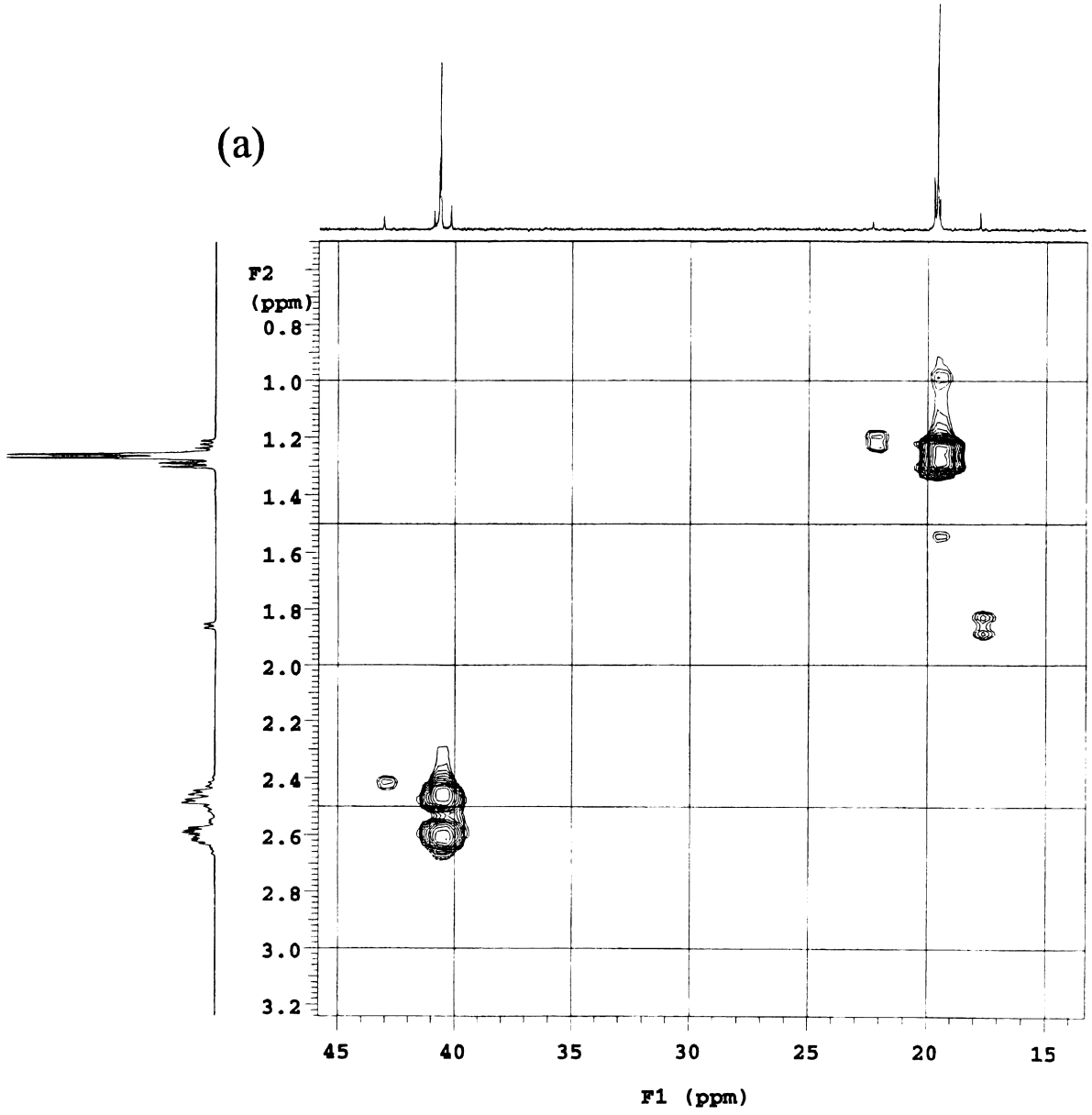

Fig. 1. HMQC spectra of a sample (PHB HC2A 149). F1 in ppm is the ^{13}C NMR trace and F2 in ppm is the ^{1}H NMR trace in each spectrum.

as shown in Fig. 1. In the HMQC 2D plots, F1 is the axis for ^{13}C and F2 is for ^{1}H spectra, respectively. Based on the assignments for ^{1}H NMR spectra and the intensities of the resonances in the ^{13}C NMR spectra, the resonances in the HMQC spectra could be assigned as follows. In Fig. 1(a), the resonances at $\delta = 19$ (F1) and $\delta = 1.25$ ppm (F2) are from $-CH_3$ and the resonances at $\delta = 41$ (F1) and $\delta = 2.43$–2.60 ppm (F2) are from $-CH_2-$. The resonances for $-CH_3$ of the propenyl end, $\underline{CH_3}$–CH=CH–, are located at $\delta = 17.6$ (F1) and $\delta = 1.85$ ppm (F2). The resonances at $\delta = 22$ (F1) and $\delta = 1.21$ ppm (F2) can be assigned for the $-CH_3$ from the normal end, HO–CH($\underline{CH_3}$)– CH_2–COO–. The resonances at $\delta = 42.8$ (F1) and $\delta = 2.42$ ppm (F2) can be assigned as the $-CH_2-$ from the hydroxyl end, HO–CH(CH_3)–$\underline{CH_2}$–COO–. In Fig. 1(b), the resonances at $\delta = 67.5$ (F1) and $\delta = 5.25$ ppm (F2) are from the backbone –$\underline{CH}$(CH_3)–. The resonances at $\delta = 64$ (F1) and $\delta = 4.19$ ppm (F2) is assigned to the –CH– from the hydroxyl end. The resonances for propenyl end group are assigned in Fig. 1(c). The resonances at $\delta = 122.5$ (F1) and $\delta = 5.80$ ppm (F2) belongs to CH_3–CH=$\underline{CH}$–COO–. The resonances at $\delta = 145$ ppm (F1) and around $\delta = 6.95$ (F2) are assigned to CH_3–$\underline{CH}$=CH–COO–. The end group –CH(CH_3)– CH_2– *C*OOH has no proton attached so that it was not assigned by COSY or HMQC. The resonance of this end group was assigned at $\delta = 172$ ppm by comparing its intensities to the intensities from –COO– in the backbone at 169 ppm. This assignment was confirmed by the fact

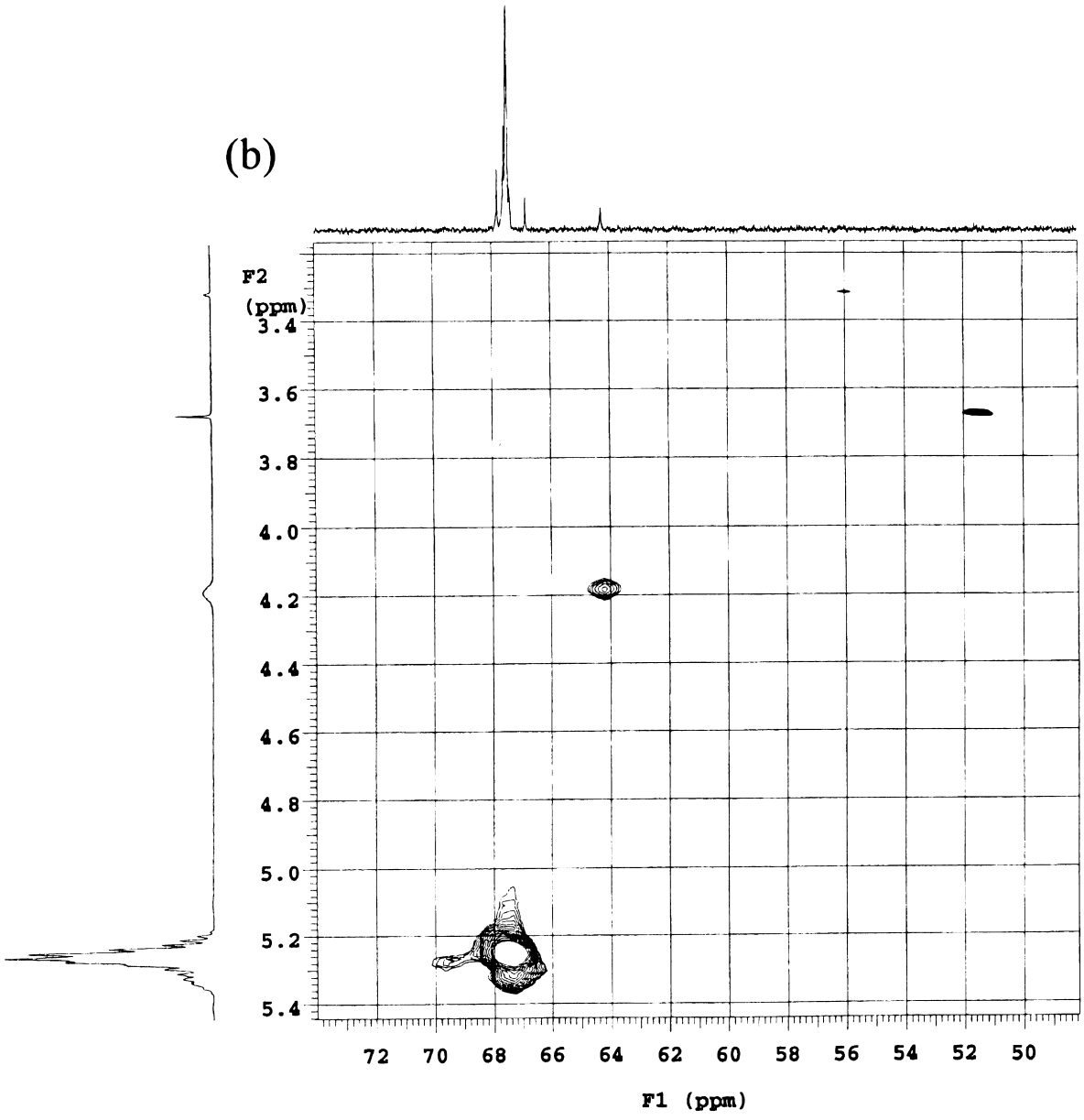

Fig. 1. (*continued*)

that the resonance at 172 ppm disappeared after PHB were converted to block copolymers by ester coupling to PEG [56].

Finally, the corresponding assignments are labelled in Fig. 2, which shows the detailed assignments of ^{1}H and ^{13}C NMR spectra. In the figure, the corresponding ^{1}H and the ^{13}C assignments are linked by lines. The assignments are listed in Table 1. Based on these assignments, we were able to calculate the molar fractions of unsaturated end (CH_3–CH=CH–) to the total ends of PHB [CH_3–CH=CH– and HO–CH(CH_3)–] by comparison of the intensities of the end groups. The number average molecular weights of the PHB samples could also be calculated based on the intensity analysis of the end groups and the backbone according to the following equation:

$$\overline{M_n} = \frac{2I_{\underline{CH},\text{backbone}}}{I_{CH_3-\underline{CH}=CH-} + I_{HO-\underline{CH}(CH_3)-}}$$

where I stands for the integral of the underlined proton in the spectrum. The results are listed in Table 2.

Unsaturated end groups and number average molecular weights of PHB could also be determined by ^{31}P NMR spectra with an internal standard according to the published method [59]. The results are listed in Table 2. However, care should be taken when this ^{31}P NMR technique is used. Reliable results are obtained only when: firstly, the equivalent molar ratio of phosphorous agent to the total –OH and

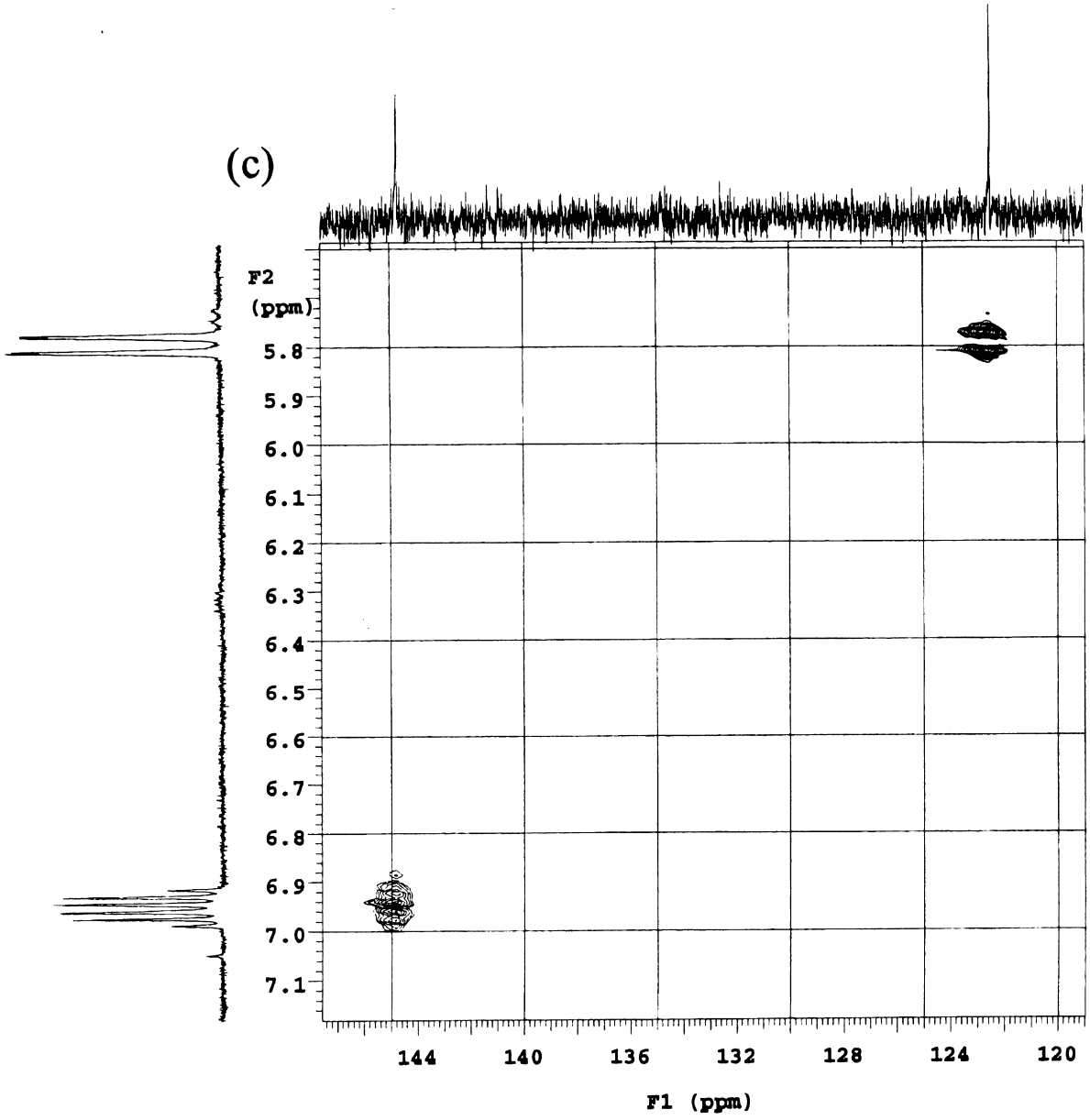

Fig. 1. (*continued*)

–COOH ends from the polymer and internal standard are larger than 2 and, secondly, the spectra should be recorded after the phosphorous agent has reacted with the sample and the standard for at least 5–10 h. Otherwise, the reaction is incomplete and side reactions may occur leading to some unassigned peaks. For a description of possible side reactions see Ref. [69].

3.3. Comments on the NMR analysis methods

It has been seen that ^{1}H and ^{13}C NMR can directly detect the unsaturated ends. Quantitative analysis can be conducted based on ^{1}H and ^{13}C NMR spectra. The ^{1}H NMR technique is more convenient, more accurate and less time consuming compared to ^{13}C NMR.

The results of the double bond molar fractions and number average molecular weights from ^{1}H and ^{31}P NMR are very close, indicating both methods are reliable. Based on the experimental procedures, ^{1}H NMR is a self-contained method and should be more reliable than ^{31}P NMR for the present purposes.

3.4. MALDI analysis

A few low molecular weight PHBs have been analysed by the MALDI technique. Fig. 3 shows a full spectrum of sample H C2A 149 ranging from mass 690 to 3000, and

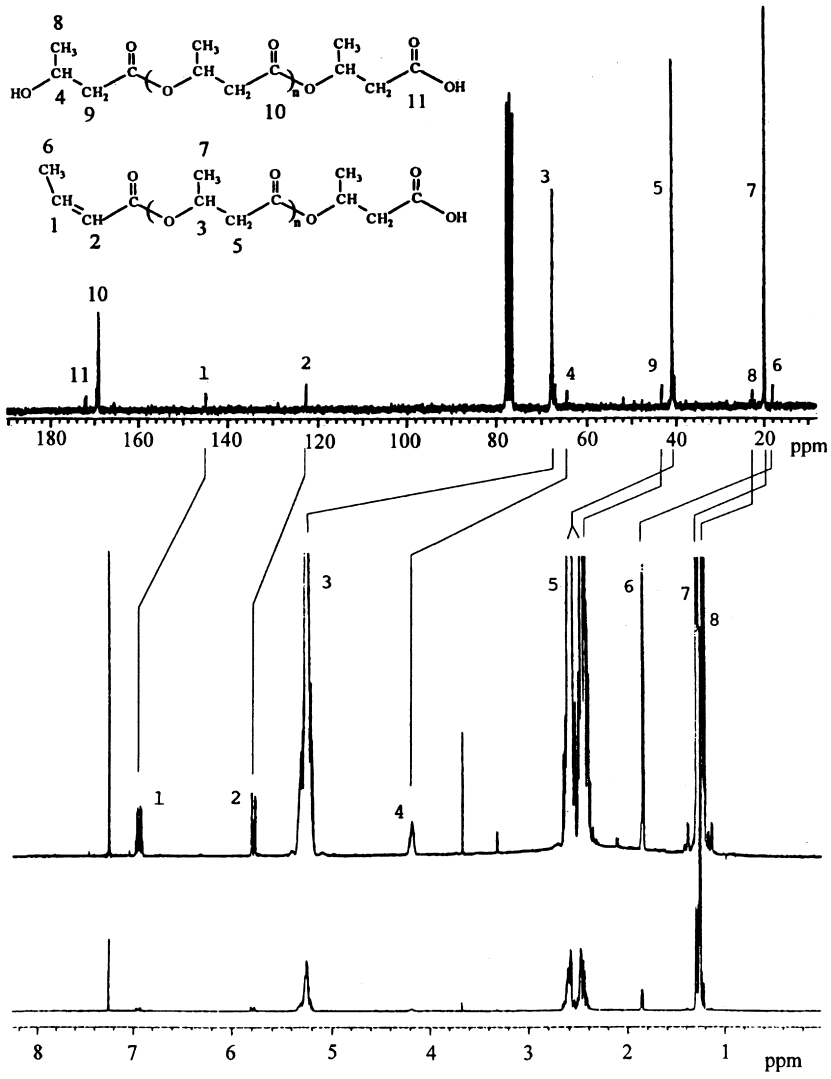

Fig. 2. The ^{1}H and ^{13}C NMR spectra of PHB HC2A 149 with the assignments indicated. The small sharp peaks marked with * are from impurities.

an expanded spectrum for one group of peaks at mass 1038–1070. The spectrum indicates clearly that most of the molecular masses are around 1000 and some around 2000, similar to the results of GPC analysis in Section 3.5. The interval of each group of peaks is 86, which is the molecular mass of one unit of the polymer, $-CH(CH_3)CH_2COO-$. The peak at 1574.6 is from a calibration standard, a cyclic poly(ether ketone). The inserted expanded spectrum in Fig. 3 shows that each group of peaks contains about 6 peaks. By the examination of each peak of the inserted spectrum, it is found that the first peak with a mass = 1038.6, equivalent to 86×12, is from a PHB molecule with an unsaturated end, $CH_3-CH=CH-$ $[CH(CH_3)- CH_2-COO]_{11}-H$, noted as (I). The second peak with a mass = 1045.4, equivalent to $86 \times 12 + 6.9$, is from the same molecule (I), however, a Li^+ ion (mass = 6.9) is added from the ionizing agent. The third peak with mass = 1052.5, equivalent to $86 \times 12 + 6.9 \times 2$, is from the molecule (I) with two Li^+ ions. The remaining three peaks show a similar pattern but they are from OH ended PHB molecules, $HO-[CH_2(CH_3)- CH-COO]_{12}- H$, noted as (II), which is 18 larger than the mass of (I). That is to say, in the expanded spectrum, the fourth peak with a mass = 1057.0 is from (II), the fifth peak with a mass = 1063.2 is from (II) plus one Li^+ and the sixth peak with a mass = 1070.7 is from (II) plus two Li^+.

Table 1
^{1}H and ^{13}C NMR spectrum assignments of PHB end groups

End group	^{1}H δ (ppm)	^{13}C δ (ppm)
HO–<u>*CH*</u>(CH_3)–	4.19 multiplet	64.2
<u>*CH*</u>$_3$–CH=CH–	1.80 doublet	18.0
CH3–CH=<u>*CH*</u>–	5.80 doublet	123.0
CH3–<u>*CH*</u>=CH–	6.95 multiplet	145.0
$-CH_2-$<u>*C*</u>OOH		172.0
HO–CH(<u>*CH*</u>$_3$)–	1.20 multiplet	22.0
HO–CH(CH_3)– <u>*CH*</u>$_2$–	2.42 multiplet	43.0

Table 2
Characterization of low molecular weight PHB by GPC and NMR

PHB sample[a]	GPC analysis		NMR analysis			
	M_w[b]	M_w/M_n[b]	C=C (mol%)		M_n	
			^1H	^{31}P	^1H	^{31}P
GC 234	980	1.13	48.0	51	970	1110
HC2A 149	990	1.11	47.0	50	1130	1200
HCb 252	1100	1.20	57.3	58	1060	1170
KC3-204	1900		52.4	48	1030	1200
	1000					
QC1-88	2500		49.6	48	2740	2930
	1100					
LP1-256	1800		55.0	66	1100	1360
	1000					
OC1-83	2000		68.2	67	1320	1350
	1050					

[a] The samples are all from Dr Hauttecoeur.
[b] From THF system calibrated by PEO.

3.5. GPC analysis

Results from GPC analysis in the THF system are listed in Table 2. The first four samples show mainly single peak characteristics but with a small shoulder on the high molecular weight side. Double peaked GPC curves were seen for a few samples, including the ones, to which no values of M_w/M_n are given in Table 2. Fig. 4 illustrates two GPC curves for two PHB samples from base hydrolysis. M_n of the samples from GPC are slightly lower than those obtained by both ^1H and ^{31}P NMR. This may be caused by using poly(oxyethylene), PEO, standards for GPC analysis. In dioxane, GPC gave similar results as those from the THF system, but resolution was poor even with 6 columns. This might indicate that dioxane is still not a very good solvent even for low molecular weight PHB at room temperature.

3.6. Mechanisms of hydrolysis of PHB

GPC curves with clear double peaks correspond to molecular weights which are approximately double, see Table 2 and Fig. 4. This double peaked phenomenon is similar to what was observed by the treatment of single crystals of PHB using gaseous methylamine [54]. This can be interpreted as a prefered hydrolysis at the chainfold surface so that the product has a DP, which is a multiple of the chain-length in a molecular stem.

A similar interpretation can be given for the data shown in Fig. 5, which is the GPC curve for the water-insoluble part of the hydrolytic products obtained by hydrolysis of a bacterial PHB (BX G08, M_w174 000) in 3 N HCl at 104°C for 15 h. Instead of a smooth curve, distinct molecular weights are observed and a given peak is more or less double that of the neighbouring peak. However, a well-defined lamellar structure was not yet developed in the original granules of PHB. Here, we propose that this experimental result can actually indicate the development of the lamellar structure in the granules during the hydrolysis course at the experimental temperature. Once the hydrolysis attack has reduce the molecular weight, lamellation is induced, as explained in our previous paper [45].

In both cases, either hydrolysis of PHB in H_2O catalysed by HCl or in CH_3OH catalysed by NaOH, the hydrolysis reactions were heterogeneous and non-random. In this situation, the hydrolysis reactions must occur at the relatively more accessible chain-fold segments at the lamellar surfaces of the crystalline material, where more flexible chain segments appear to meet the condition of a tetrahedral intermediate required for hydrolysis of esters [34]. The result is a non-continuous molecular weight distribution, which allows sharp fractionation and in this case preparation of gram quantities of the product.

The mechanism of double bond formation from the hydrolysis process should be distinguished from that in the thermal degradation of PHB. The former should be purely from dehydration of the hydroxyl end, HO–$CH(CH_3)$– CH_2–COO–. by β-elimination after the chains are broken during hydrolysis. This is also supported by the experimental results of Athlan et al. [46] In the case of thermal degradation, the double bonds are formed at the same time as the PHB chains are broken as indicated in Scheme 2.

3.7. Dependence of melting point and lamellar thickness on the molecular weight of PHB

PHB and PHB oligomers have a lamellar crystalline structure [57,70–74] when precipitated from dilute solution or when prepared as single crystals. Study of lamellar thickness for PHB samples with different molecular weight was the subject of a previous paper, [57] using small angle X-ray diffraction. In the present paper, a few more data points are added and the dependence of lamellar thickness for PHB on molecular weight is plotted in Fig. 6. As can be seen, the lamellar thickness of PHB crystals increases rapidly to ~40 Å at a molecular weight of 2000. Beyond a molecular weight of 2000, the lamellar thickness plateaus at a value of ca. 48 Å, indicating the development of chain folding in PHB crystals. The rapid increase of lamellar thickness in the low molecular weight region suggests extended chain crystallization [57].

Fig. 7 shows a plot of melting point against molecular weight of PHB. The melting points measured by an optical method are close to those from DSC. The rapid increase of T_m with the number average molecular weight of PHB is due to increased crystal thickness. Beyond 20 000, the dependence of the T_m on M_n is barely detectable, in keeping with the data in Fig. 6.

Fig. 8 shows a plot of melting points (T_m) against reciprocal lamellar spacings (1/L) for PHB samples. The melting points fall onto a straight line with a large slope for those samples with molecular weights from about 700 to 15 000.

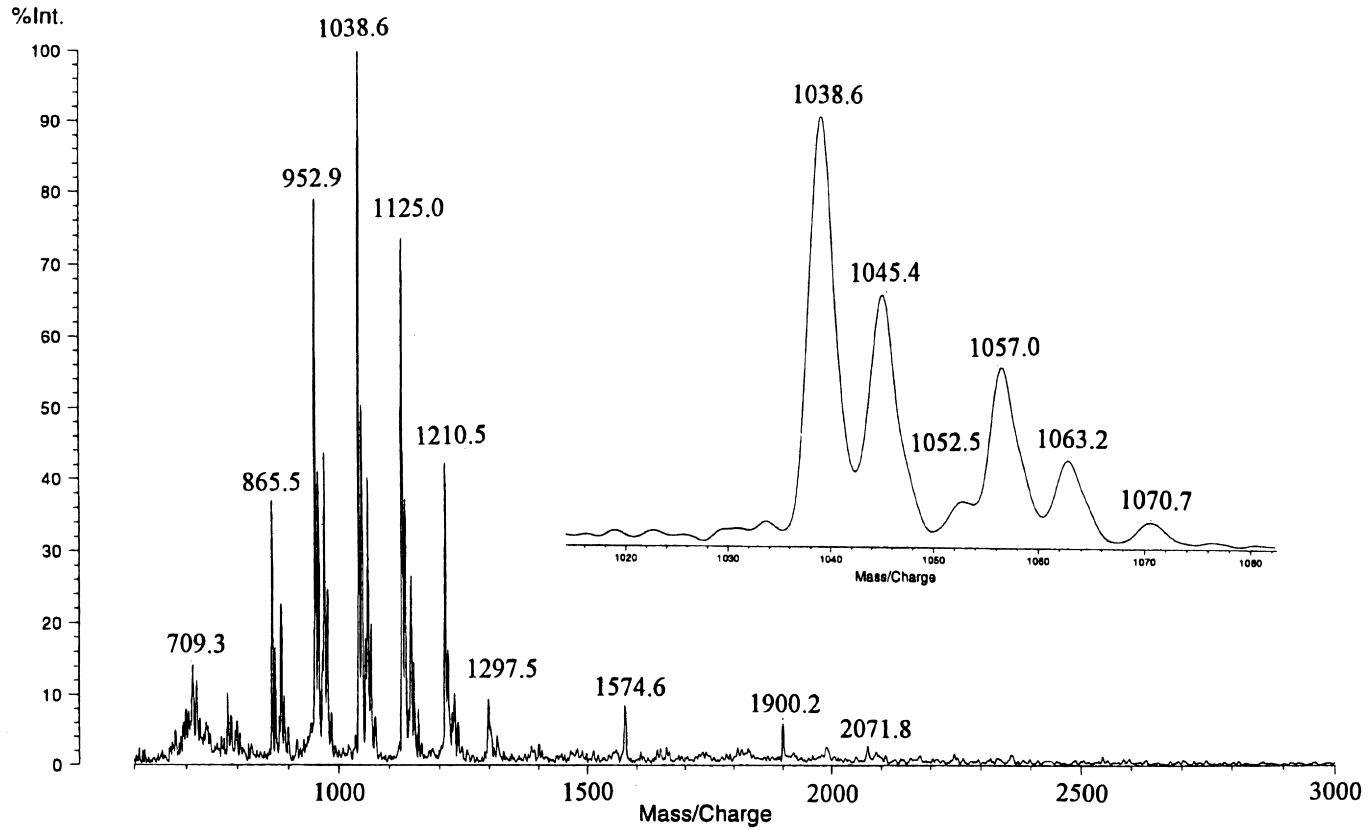

Fig. 3. MALDI spectra for a PHB sample (PHB HC2A 149). The inset spectrum is the expanded area for the group of peaks from 1038 to 1070.

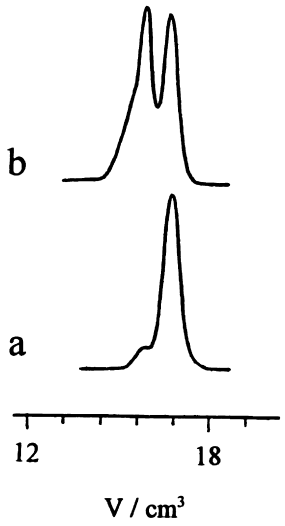

Fig. 4. The GPC curves of two low molecular weight PHB samples analysed in THF. The results are in Table 2. (a) sample HC2A 149; (b) sample OC1-83.

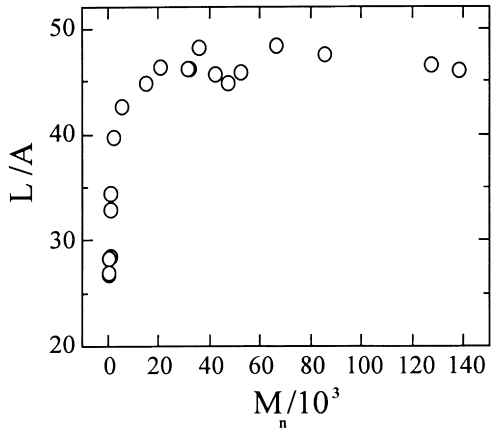

Fig. 6. The plot of lamellar thickness against the molecular weight of PHB.

The data points for the high M_n PHB (M_n from 15 000 to 138 000, 7 data points) are crowded in a small region in Fig. 8, because the lamellar thickness does not increase with further increase in molecular weights. All the samples were precipitated from about 1 to 2% chloroform solution under similar conditions and pressed into discs for SAXS studies.

The theoretical equation for the melting temperature T_m, for lamellar single crystals is:

$$T_m = T_m^0(1 - \frac{2\sigma}{\Delta H_f^0 L})$$

where σ is the end surface free energy (J m^{-2}), ΔH_f^0 the enthalpy of fusion (J m^{-3}) per mole of repeat units, L the lamellar thickness (m) and T_m^0 is the melting point of an infinitely thick crystal. The greater slope of T_m against $1/L$ from these low molecular weight samples is due to the surface energy effect. For low molecular weight samples with extended chain, the surface to volume ratio is high and the surface may include a hydroxyl, carboxyl or double bond end groups leading the higher surface energy than for the high molecular weight chains with regular folding. When data for the latter are used to obtain the T_m^0, a value of ~206°C is found. This value is similar to the estimated T_m^0 (197°C) from the plot of melting temperature against the crystallization temperature [74]. Another way to estimate T_m^0 is by plotting the annealing temperature against the reciprocal lamellar thickness [57,70]. The open circles in Fig. 8 are the result of an annealing study for a PHB single crystal sample with $M_n = 32\ 360$, and the plot extrapolates to a T_m^0 of about 200°C [57].

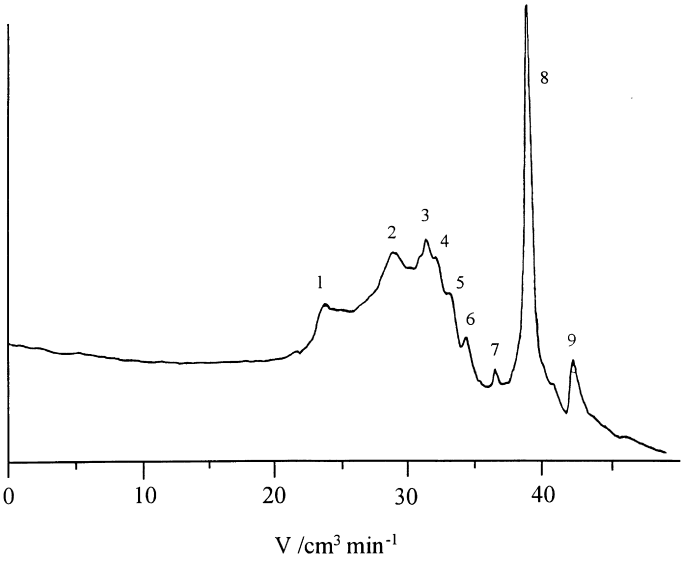

Fig. 5. The GPC curve of a hydrolyzed PHB sample analysed by a $CHCl_3$ system. The relative weight average molecular masses for the peaks are 1, 89 400; 2, 5500; 3, 2800; 4, 2100; 5, 1540; 6, 900; and 7,340. The peaks 8 and 9 are from solvent. The calibration was against PS standards.

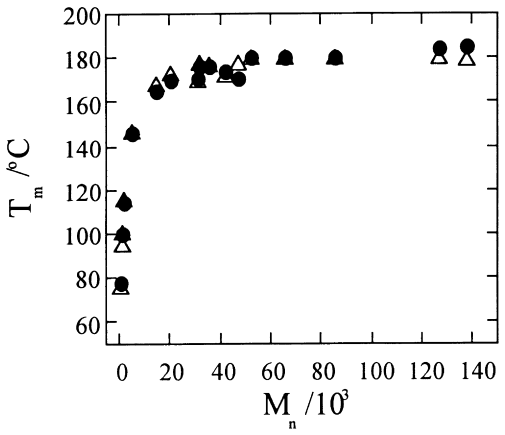

Fig. 7. The plot of melting point against M_n of PHBs. The filled circles are from DSC measurement and the triangles are from optical measurement.

4. Summary and conclusion

^{1}H, ^{13}C and ^{31}P NMR techniques have been used to characterize low molecular weight PHB samples. MALDI is also a useful technique to analyse low molecular weight PHB samples. Based on these analyses of low molecular weight PHBs resulting from basic and acidic hydrolysis, the heterogeneous hydrolysis and saponification of PHB are suggested to occur at the chain folding surfaces of PHB lamellae. This selective site of hydrolysis explains the narrow spread in molecular weight of the various hydrolysed samples. The unsaturated end group is formed by the dehydration of the chain ends after the ester hydrolysis.

The use of alkaline and acid hydrolysis of bacterial PHB to produce low molecular weight product is advantageous for optically active specialty polymer synthesis. Remarkably narrow molecular weight material obtained is valuable for molecular design of block and graft copolymers. The presence of double bonds at the chain ends can be used advantageously in a variety of reaction schemes.

Lamellar thickness and melting point increase rapidly with molecular weight for the low molecular weight PHB.

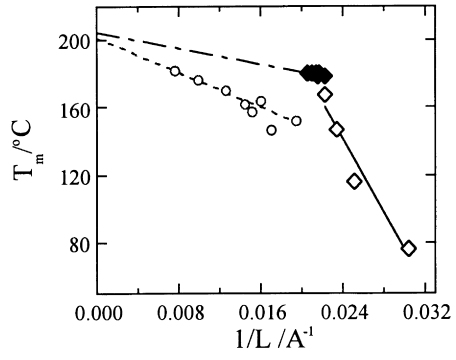

Fig. 8. The plot of melting point against reciprocal lamellar thickness of PHB. The open diamond symbols are from the molecular weight range of 700–15 000; the filled symbols are from the molecular weight range of 20 000–138 000. The open circles are the comparison plot of annealing temperature against $1/L$ for a PHB with $M_n = 32\ 360$.

The initial steep slope of the melting point against reciprocal lamellar thickness for low molecular weight PHB indicate a surface energy effect, which is caused by a concentration of the end groups at the crystal surface.

Acknowledgements

The authors would like to acknowledge financial support from NSERC, Labopharm Inc. and Xerox Corp. Dr K. Okamura is thanked for supplying the SAXS data and most of the melting points of the samples. Dr B. Hauttecoeur is thanked for the gifts of the low molecular weight samples. MALDI experiments were done by Ms A. Hlil in Dr A. Hay's laboratory.

References

[1] Hocking PJ, Marchessault RH. In: Griffin GIL, editor. Chemistry and technology of biodegradable polymers. London: Blackie Academic & Professional, 1994. p. 48.
[2] Marchessault RH. TRIP 1996;4:163.
[3] Doi Y. Microbial polyesters. New York: VCH, 1990.
[4] Hammond T, Liggat JJ. In: Scott G, Gilead D, editors. Degradable polymers. London: Chapman & Hall, 1995. p. 88.
[5] Steinbuechel A, Valentin H. FEMS Microbiol Lett 1995;128:219.
[6] Steinbuechel A. In: Byrom D, editor. Biopolymers. London: Macmillan, 1991. p. 123.
[7] Seebach D, Roggo S, Zimmermann J. In: Bartmann W, Sharpless KB, editors. Stereochemistry of organic and bioorganic tansformations wrkshop conferences, Hoechst, vol. 17. Verbagsgesellschaft mbh VCH, 1987. p. 87.
[8] Mueller HM, Seebach D. Angew Chem Int Ed Engl 1993;32:477.
[9] Holmes PA. In: Basset DC, editor. Developments in crystalline polymers. New York: Elsevier, 1988. p. 1.
[10] Braunegg G, Lefebvre G, Genser KF. J Biotech 1998;65:127.
[11] Doi Y, Fukuda K, editors. Biodegradable plastics and polymers. Amsterdam: Elsevier, 1994.
[12] Proceedings of International Symposium on Biological Poly(hydroxyalkanoates), Sept. 9–11, 1998, Riken, Japan.
[13] Doi Y, Kitamura S, Abe H. Macromolecules 1995;28:4822.
[14] Barham PJ, Keller A, Otun EL, Holmes PA. J Mater Sci 1984;19:2781.
[15] Kumagai Y, Kamesawa Y, Doi Y. Macromol Chem 1992;193:53.
[16] Abe H, Matzubara I, Doi Y, Hori Y, Yamaguchi A. Macromolecules 1994;27:6018.
[17] Tomasi G, Scandola M, Briese BH, Jendrossek D. Macromolecules 1996;29:507.
[18] Hocking PJ, Revol JF, Marchessault RH. Macromolecules 1996;29:2467.
[19] Hocking PJ, Marchessault RH, Timmins MR, Scherer TM, Lenz RW, Fuller RC. Macromol Chem Rapid Commun 1994;15:447.
[20] Hocking PJ, Timmins MR, Scherer TM, Lenz RW, Fuller RC, Marchessault RH. J Macromol Sci Pure Appl Chem 1995;A32:889.
[21] Hocking PJ, Marchessault RH, Timmins MR, Scherer TM, Lenz RW, Fuller RC. Macromolecules 1996;29:2472.
[22] Nobes GAR, Marchessault RH, Chanzy H, Briese BH, Jendrossek D. Macromolecules 1996;29:8330.
[23] Iwata T, Doi Y, Kasuya KI, Inoue Y. Macromolecules 1997;30:833.
[24] Morikawa H, Marchessault RH. Can J Chem 1981;59:2306.
[25] Grassie N, Murray EJ, Holmes PA. Polym Degrad Stab 1984;6:47.
[26] Grassie N, Murray EJ, Holmes PA. Polym Degrad Stab 1984;6:95.
[27] Grassie N, Murray EJ, Holmes PA. Polym Degrad Stab 1984;6:127.

[28] Tighe BJ. In: Scott G, editor. Developments in polymer degradation. Bearking, UK: Applied Science, 1984. p. 50.
[29] Kunioka M, Doi Y. Macromolecules 1990;23:1933.
[30] Kopinke FD, Remmler M, Mackenzie K. Polym Degrad Stab 1996;52:25.
[31] Williams RJ, Lehrle RS. Macromolecules 1994;27:3782.
[32] Hammond T, French C, Willams R, Lerle RS. Macromolecules 1995;28:4408.
[33] Melchiors M, Keul H, Hoecker H. Macromolecules 1996;29:6442.
[34] March J. Advanced organic chemistry: reactions, mechanisms, and structure. New York: McGraw–Hill, 1968.
[35] Lemoigne M. CR Acad Sci 1925;180:1539.
[36] Holland SJ, Holly AM, Yasin M, Tighe BJ. Biomaterials 1987;8:289.
[37] Miller ND, Williams DF. Biomaterials 1987;8:1290.
[38] Holland SJ, Yasin M, Tighe BJ. Biomaterials 1990;11:206.
[39] Yasin M, Holland SJ, Tighe BJ. Biomaterials 1990;11:451.
[40] Korsatko W, Wabnegg B, Tillian HM, Braunegg G, Lafferty RM. Pharm Ind 1983;45:1004.
[41] Korsatko W, Wabnegg B, Tillian HM, Egger G, Pfragner R, Walser V. Pharm Ind 1983;46:952.
[42] Doi Y, Kanesawa Y, Kawaguchi Y, Kunioka M. Macromol Chem Rapid Commun 1989;10:227.
[43] Kanesawa Y, Doi Y. Macromol Chem Rapid Commun 1990;11:679.
[44] Doi Y, Kanesawa Y, Kunioka M. Macromolecules 1990;23:26.
[45] Lauzier C, Revol JF, Debzi EM, Marchessault RH. Polymer 1994;35:4156.
[46] Braud C, Devarieux R, Garreau H, Vert M. J Environ Polym Degrad 1996;4:135.
[47] Athlan A, Braud C, Vert M. J Environ Polym Degrad 1997;5:243.
[48] Hauttecoeur B, Jolivet M, Gavard R. CR Acad Sci Paris Series D 1972;274:2729.
[49] Hauttecoeur B, Jolivet M, Gavard R. CR Acad Sci Paris Series D 1975;280:2801.
[50] Gavard R, Dahinger A, Hauttecoeur B, Reynaud C. CR Acad Sci Paris 1966;263:1273.
[51] Gavard R, Dahinger A, Hauttecoeur B, Reynaud C. CR Acad Sci Paris 1966;263:1640.
[52] Gavard R, Reynaud C, Hauttecoeur B, Dahinger A. CR Acad Sci Paris Series D 1967;265:1557.
[53] Hauttecoeur B, Jolivet M, Gavard R. CR Acad Sci Paris Series C 1972;274:1957.
[54] Welland EL, Stejny J, Halter A, Keller A. Polymer Commun 1989;30:302.
[55] Yalpani M, Marchessault RH, Morin FG, Monasterios CJ. Macromolecules 1991;24:6046.
[56] Marchessault RH, Yu GE. Division of polymeric materials: science and engineering, ACS meeting at Anaheim, CA, March 21–25, 1999.
[57] Marchessault RH, Coulombe S, Morikawa H, Okamura K, Revol JF. Can J Chem 1981;59:38.
[58] Coulombe S, Schauwecker P, Marchessault RH, Hauttecoeur B. Macromolecules 1978;11:279.
[59] Spyros A, Argyropoulos DS, Marchessault RH. Macromolecules 1997;30:327.
[60] Wang YF, Paventi M, Chan KP, Hay AS. J Polym Sci Polym Chem Ed 1996;34:2135.
[61] Terada M, Marchessault RH. Proceedings of ISBP 1998. Tokyo, Int J Biol Macromol, in press.
[62] Doi Y, Knioka M, Nakamura Y, Soga K. Macromolecules 1986;19:1274.
[63] Doi Y, Knioka M, Nakamura Y, Soga K. Macromolecules 1986;19:2860.
[64] Kamiya N, Yamamoto Y, Inoue Y, Chujo R, Doi Y. Macromolecules 1989;22:1676.
[65] Bloembergen S, Holden DA, Bluhm TL, Hamer GK, Marchessault RH. Macromolecules 1989;22:1656.
[66] Bloembergen S, Holden DA, Hamer GK, Bluhm TL, Marchessault RH. Macromolecules 1986;19:2865.
[67] Gross RA, DeMello C, Lenz RW, Brandl H, Fuller RC. Macromolecules 1989;22:1106.
[68] Kumagai Y, Doi Y. J Environ Polym Degrad 1993;1:81.
[69] Archipov Y, Argyropoulos DS, Bolker HI, Heitner C. J Wood Chem Technol 1991;11:137.
[70] Okamura K. PhD thesis, SUNY College of Forestry, Syracuse, NY, 1967.
[71] Cornibert J, Marchessault RH. J Mol Biol 1972;71:735.
[72] Yokouchi M, Chatani Y, Tadokoro H, Teranishi K, Tani H. Polymer 1973;14:267.
[73] Alper R, Lundgren DG, Marchessault RH, Cote WA. Biopolymers 1963;1:545.
[74] Barham PJ, Keller A, Otun EL. J Mater Sci 1984;19:2781.